Journal of Applied Research in Water and Wastewater
E-ISSN: 2476-6283
Journal homepage: https://arww.razi.ac.ir

# Hargreaves-Samani method: Estimation of historical annual, seasonal, and monthly Reference Evapotranspiration (ETo) in Dadu District, Pakistan

**Shoukat Ali Shah***

*Institute of Water Resources Engineering and Management, Mehran University of Engineering and Technology, Jamshoro, Sindh, Pakistan.*

## GRAPHICAL ABSTRACT

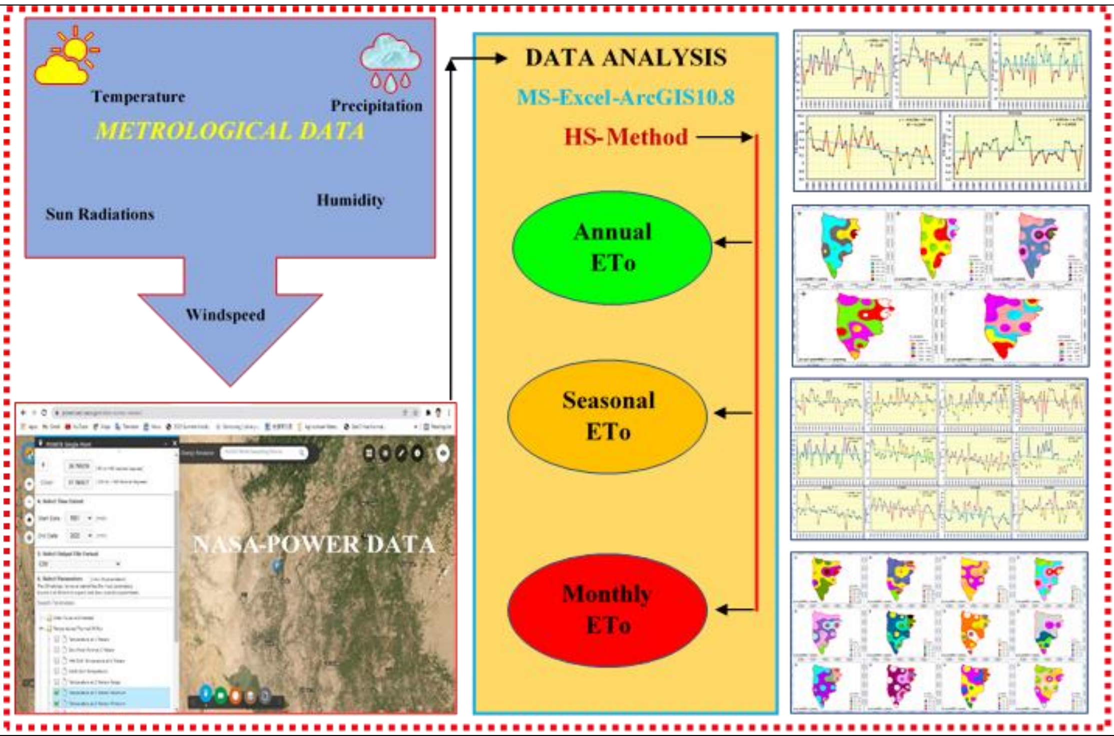


## ARTICLE INFO

**Article history:**
Received 7 February 2022
Reviewed 14 April 2022
Received in revised form 20 June 2022
Accepted 25 June 2022
Available online 27 June 2022

**Keywords:**
Reference evapotranspiration
IDW interpolation
NASA-POWER
Hargreaves-Samani

**Article type:** Research Article

© The Author(s)
Publisher: Razi University

## ABSTRACT

Reference Evapotranspiration (ETo) counted as the main factor for assessing the amount of water, needed for crops as well as for the planning of water resources management. Several techniques, methods, and equations have been used for computing ETo. Thus, required weather data sets are the main challenge for evaluating this factor. FAO Penman-Monteith is the most popular technique to determine the ETo. The FAO 56-PM equation requires accurate weather data like air temperature, humidity, solar radiations, and wind speed. Unfortunately, not all these data are possible to reach easily on the station's side. Therefore, FAO 56 recommended another equation namely Hargreaves-Samani (HS) equation when sufficient weather data may not be available to estimate ETo by FAO56-PM. In the context of this, this study aimed to estimate ETo using the HS equation. For this purpose, historical annual, seasonal, and monthly temperature and wind data were collected from 1981 to 2020 using 'The Prediction of Worldwide Energy Resources (POWER)' web portal. It is concluded that the HS method in conjunction with the POWER datasets and spatially mapping with IDW interpolation gave reliable and accurate results of ETo. This technique gives an idea of water losses in a district and demonstrates a trend of historical annual, seasonal, and monthly ETo.

### 1. Introduction

Reference Evapotranspiration (ETo) assists as an essential parameter for hydrological modeling, hydrological balance studies, water management, designing and schedu ling of irrigation water, working in flooded and rainfed conditions, and watershed hydrology allied with environmental and metrological factors. Surplus knowledge with ETo is crucial while managing water management problems. Such as the demand for water for different purposes i.e., irrigation, farming, and industrial purposes (Thornthwaite. 1948). ETo offers potential advantages especially irrigation management in different cropping seasons, patterns, irrigation efficiency, and water productivity. Hence,

*Corresponding author Email: sarkar.sain151@gmail.com

How to cite: S.A. Shah, Hargreaves-Samani method: Estimation of historical annual, seasonal, and monthly Reference Evapotranspiration (ETo) in Dadu District, Pakistan, *Journal of Applied Research in Water and Wastewater*, 9 (1), 2022, 30-39.

the exact estimation of ETo is playing a key role in improving irrigation efficiency, water reuse, and seepage control (Shiri. 2019). The metrologists used direct and indirect different existing methods and equations to determine ETo. The direct estimation from a reference crop including perennial grass and indirect methods is figured from weather data i.e., temperature, radiation, wind speed, and various models.

According to Allen et al. (1998), the FAO has recommended Penman-Monteith (FAO 56-PM) equation which is widely used for ETo estimation and is known as the most accurate method using different climate data (Yamac. 2018; Rodrigues and Braga. 2021a; Gentilucci et al. 2021). Though the method has some drawbacks, it needed excess weather data i.e., temperature, humidity, wind speed, solar radiation, etc. Unfortunately, these all data cannot be obtained from many of the regions through metrological stations in developing countries Tabari et al. (2013). Thus, counter many difficulties to estimate ETo by this method. If the accessibility of weather data collection in any region is available then FAO PM-56 equation is advisable (Droogers and Allen. 2002). If the availability is limited, a temperature-based equation should be employed recommended by FAO, called Hargreaves and Samani (HS) equation (Hargreaves and Samani. 1985a). HS requires only temperature for ETo estimation. This equation can be used for remote areas where the unavailability of data and temperature data are the most commonly recorded metrological data in every station. This temperature-based ETo equation is derived from air temperature, humidity term, day-night length, and some other factors which make the equation more specific and accurate (Xu and Singh. 2002).

Several online free of charge platforms provide historical datasets available in different periods of daily, monthly, and annual analyzed data Kobayashi et al. (2015). Due to the easily operated, and user-friendly, one that attracts attention is the ‘National Aeronautics and Space and Administration’, ‘The Prediction of Worldwide Energy Resources’ (NASA-POWER) Chandler et al. (2013). The POWER project portal provides historical metrological data. The project was developed with the support of NASA Earth Sciences. The main purpose is to provide renewable energy, sustainable buildings, and agroclimatology data. However, easily operated NASA-POWER, when compared with other platforms, allows to easily approach data. The data in three forms since it is existing, i. a single point, (single ‘N’ Longitude and ‘E’ Latitude), it provides historical data based on the registered coordinate, selected by the operator, ii, it provides a regional endpoint, historical dataset based on a bounding box of ‘E’ latitude and ‘N’ longitude demarcated by the operators, and iii, the global point that returns historical climatological average for the whole globe (Rodrigues & Braga, 2021b). If data evidence is accurate, and easily approached when compared to other weather data providers, permits any user to simply have an approach to near real-time and wide-ranging climate data from any place around the globe.

The spatial interpolation Inverse Distance Weighted (IDW) performance has the purpose of defining ETo over different types of land use cover of the study area. The method has been calculated for different time steps, the monthly, annual, and seasonal level ETo for 39 years. Based on the findings, and with specific attention paid to the availability of data and reviewing the past literature, the chosen method HS, and its interpolation by running IDW could be the better choice to achieve the targets. Based on the above-mentioned literature and description, the creativity and purpose of the current study aimed to estimate the historical annual, seasonal, and monthly ETo using the HS equation and mapping ETo in the Dadu district.

## 2. Materials and methods

### 2.1. Study area

The study area Dadu district is located at 26º 06’ 35” to 27º 26’ 20” north latitude and 67º 07’ to 68º 02’ 17” east longitude. The district is situated in the west of Sindh. The district has bordered by the North of Kamber Shadadkot, on the East Larkana district, and Shaheed Benazeerabad district, on the West Kirthar mountains and Baluchistan and the South Jamshoro district (Fig. 1). The total geographical area of Dadu is 8035 km$^2$ (4992.096 miles). The district comprises 4 talukas viz.; Dadu, Mehar, Khairpur Nathan Shah, and Johi. Pakistan Bureau of Statistics counted the population of the district as about 1550266 PBS, (2017) in which urban population is about 25 % and rural 75 % of the total population exists. The Indus River flows along the boundary of Dadu from north to south. Manchar Lake is a second natural reservoir in the district and is usually used for fish breeding.

The district is divided into three parts namely, i. The Kohistan, and Kachho area, ii. The barrage zone, and iii. The low land riverine area. Dadu is intensively hot in summer and cold in winter. The temperature was recorded between 17℃ to 46℃. Annual rainfall has been noted at about 120mm. Agriculture is the livelihood of the people. Crop patterns, sowing, and harvesting time are different due to regional variations in temperature, soil texture, varieties, availability of irrigation water, etc. Agriculture is categorized as major-minor crops. Wheat, cotton, rice, and sugarcane are the major crops, and barely, jowar, gram, and mustard fall as minor crops.

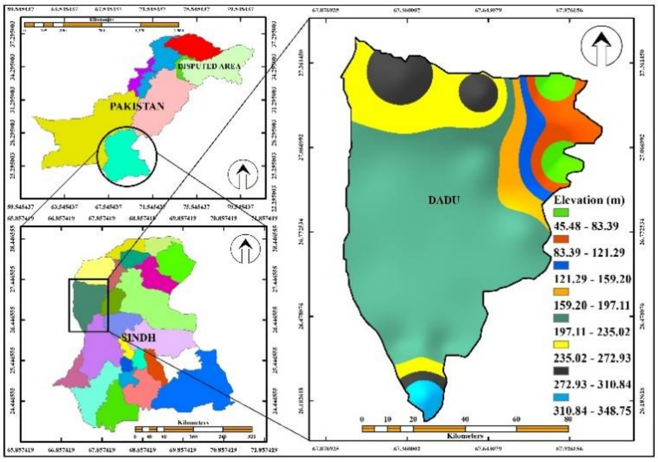


**Fig. 1**. Administrative map of Dadu district, Sindh, Pakistan.

### 2.2. Data collection and processing

To achieve the targets, the shape file of the Dadu was converted into a KML file. Thirteen points were created by given names as D1, D2 D3 up to D13 (Here D shows Dadu) (Fig. 2). For the accuracy of metrological data, all the control points covered the whole district. The recorded metrological data from 1981 to 2020 including monthly and annual data of temperature (maximum and minimum), wind speed data (2 m), and elevation data were acquired from an online web portal ‘The Prediction of Worldwide Energy Resources (POWER)’ project (Fig. 3). Particularly, it provides solar and metrological datasets from NASA for support of renewable energy, building energy efficiency, and agricultural needs. A large amount of data was exported to MS-Excel for more preparation. Firstly, the data was compiled and then interpolated each control point data for more accuracy in the analyzed results. The control point's name, latitude, longitude, annual average, and seasonal average (winter, summer, spring, and autumn) (Table.1).

### 2.3. Evaluation of Hargreaves-Samani equation

The ETo was computed by the HS equation (Hargreaves and Samani. 1985b). The method is frequently applied for computing ETo (mm/unit time), requires only temperature (minimum and maximum), and extra-terrestrial radiations that might be found every metrological stations. To achieve the targets, an MS Excel auto calculator was developed for computing ETo using the HS equation (Fig. 4). Compiled average data of (minimum and maximum) temperature and average (minimum and maximum) wind was exported one by one for accurate results of ETo.

$$ETo = 0.0023\frac{Ra}{\lambda}\sqrt{(Tmax - Tmin)}(T + 17.8) \quad (1)$$

where, the coefficient 0.0023 is an empirical coefficient, Ra is the extraterrestrial radiation (mm/unit time) computed according to Allen et al., (1998) and λ is the latent heat of vaporization (MJ/kg) for the mean air temperature T (°C).

$$\lambda = 2.501 - 0.002361.\mathrm{T} \quad (2)$$

**Table 1.** Illustrate seasonal information.

| Season name | Months |
|---|---|
| Winter | January, February, and December |
| Spring | March, April, and May |
| Summer | June, July, and August |
| Autumn | September, October, and November |

### 2.3. Interpolation (IDW)

The historic data of 39 years of annual, seasonal, and monthly graphs for ETo was prepared in MS Excel. Analyzed data further exported in ArcGIS 10.8 for accurate visualization. The control points D1 to D13 were added to ArcGIS 10.8, and from their latitude and longitude, the rest of the annual, seasonal, and monthly data could then be interpolated using IDW within the location point’s attribute Table. The IDW function was utilized to interpolate annual, seasonal, and each month, with the result being one map of annual, four maps of seasonal and twelve maps of average results of ETo throughout the entire district were developed.

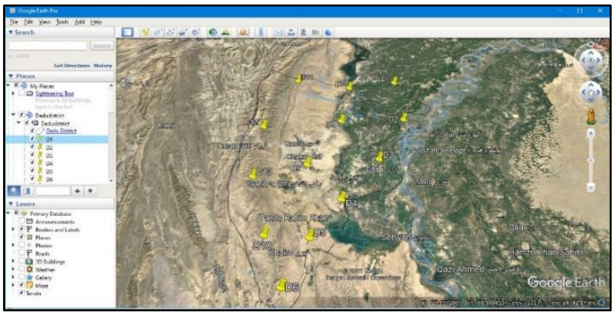

**Fig. 2.** Control points D1 to D13.

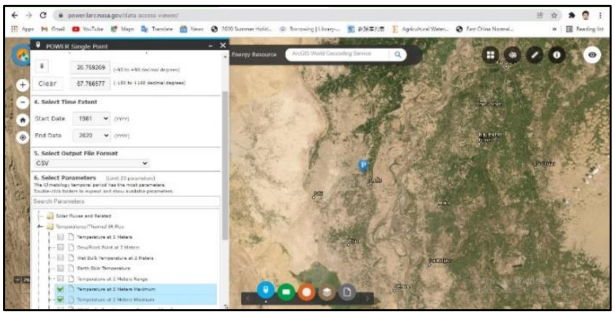

**Fig. 3.** An overview of the prediction of worldwide energy resources (POWER).

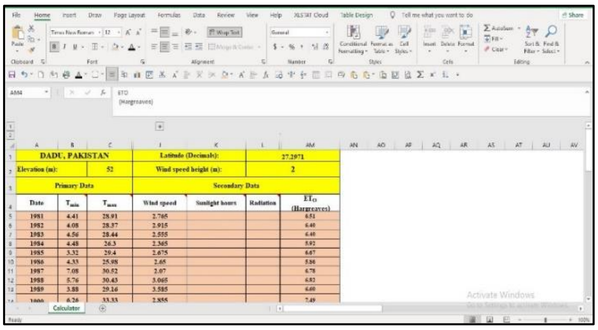


**Fig. 4.** Auto computing calculator of ETo (mm/day) in the MS Excel sheet.

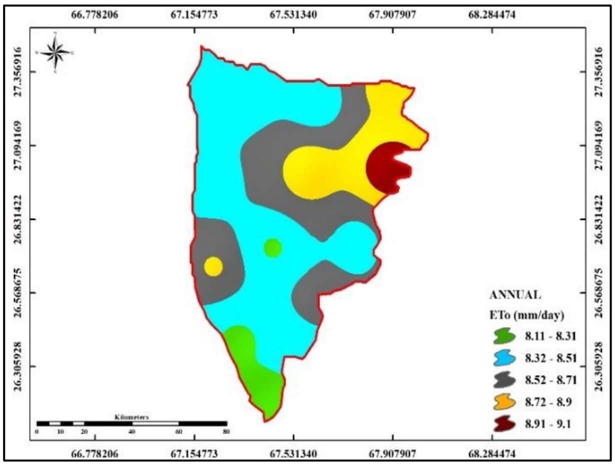


**Fig. 5.** Annual ETo over the district.

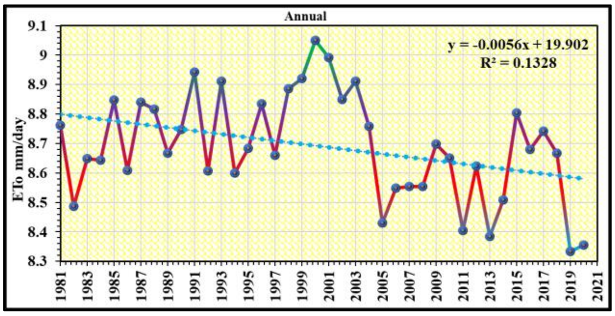


**Fig. 6.** Graph showing annual ETo from 1981-2021over the district.

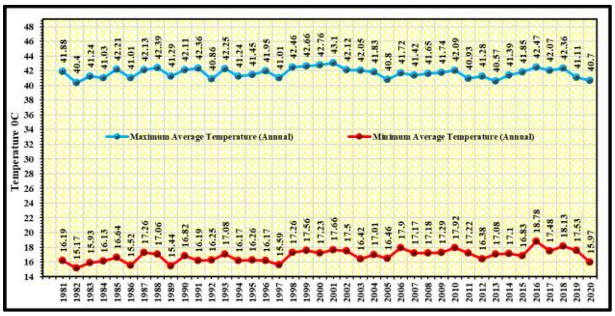


**Fig. 7.** The annual maximum average temperature from 1981-to 2020.

## 3. Results and discussion

### 3.1. Estimation of historical annual and seasonal ETo

The difference in climatic parameters such as surface temperature, wind, precipitation, wind speed, and shifting of low- and high-pressure cells from one portion to the ocean and then towards the other portion of the world causes the variation in the evapotranspiration. The variation and roughness of the topography of the mountains is also the major factor to deflect the wind from one direction to another direction, also producing a difference in the wind speed. It has been noted that the plain areas of the district have high ETo as compared to hilly areas in all the seasons. The historical ETo was computed through the derived equation of HS by using 39 years of temperature and wind data. The data were carefully screened from the POWER project on 13 different points. The annual and seasonal ETo results are demonstrated in (Table 2).

#### 3.1.1. Annual reference evapotranspiration

The annual average ETo was computed to range from 8.76 mm/day in 1981 and 8.35mm/day in 2020. The maximum annual ETo depicted in 2000 was 9.05mm/day. ETo demonstrated a trend line of ETo $R^2$=0.132 showing there is a decrease in annual ETo from the previous 39 years (Fig. 6). The visual inspection of maximum ETo in (Fig. 5) shows 8.72-8.9 mm/day over the vegetative area of the district. The highest temperature was recorded in 2001 at 43 °C and the lowest temperature at 15 °C in 1982 (Fig. 7).

#### 3.1.2. Winter reference evapotranspiration

The winter season ETo ranged from 6.64 mm/day in 1981 and 7.15 mm/day in 2020 (Table 2). The highest ETo computed in 2000 was 7.84 mm/day. It was observed that in 2000 there was an increase in temperature and a drought period. The $R^2$=0.132 was computed in the winter season (Fig. 9). The trend line showed that ETo was increased in the winter season. However, in the winter season evapotranspiration has been low due to seasonal variations such as short days, high humidity rate, cold wind, decrease in temperature, fogs, and the highest precipitation rate Khan and Hassan, (2017). Hilly areas show maximum ETo as 7.02 mm/day to 7.87 mm/day (Fig. 8). The historical average temperature graph shows that the lowest temperature was recorded at 3.1 °C in 1984, whereas the highest surface temperature was recorded at 34.21°C in the 2000 year (Fig. 10). The vegetative area in (Fig. 8) depicted that moderate ETo was recorded between 6.7 mm/day to 6.85 mm/day during the whole winter season.

#### 3.1.3. Spring reference evapotranspiration

The results of ETo in the Spring season ranged from 10.9mm/day in 1981 and 8.96mm/day in 2020. The highest values of ETo were calculated over some portions of the vegetation as 10.2 mm/day to 10.5 mm/day (Fig.11). The linear coefficient graph and the line showed $R^2$=0.0003 and observed a decrease in the ETo (Fig.12). This weak coefficient is due to continued decreases in the wind as well as low surface temperature over the district. The less rainfall in the district and a shortage of surface water in 2010 and 2017. Indeed, 2010 was the year of flood in the region. The Spring season months counted are March, April, and May. In these months, the temperature and wind fluctuate as normal. The climate of these months adds up as well in the region because of normal temperature and humidity. Particularly, the March month surface temperature scale was recorded between 12 °C to 47 °C (Fig. 13).

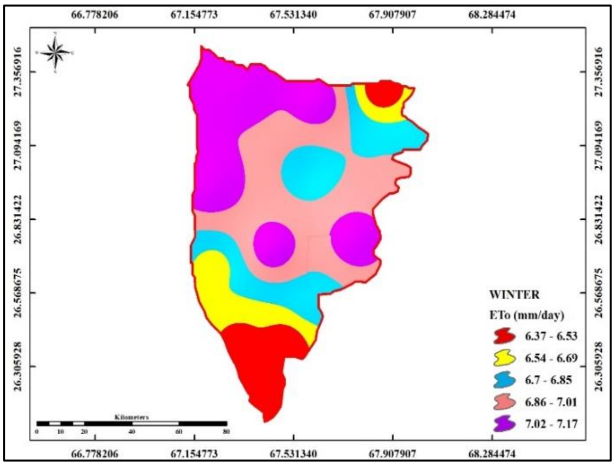


**Fig. 8.** Winter season ETo over the study area.

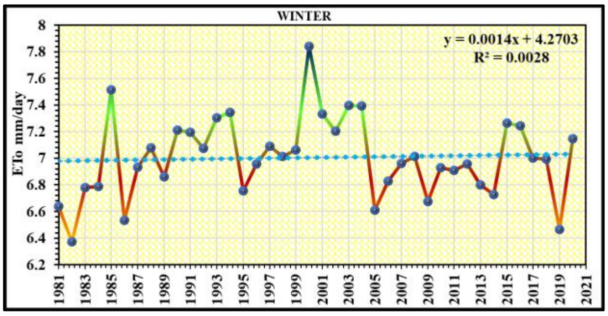


**Fig. 9.** Graph showing Winter season ETo from 1981-2021.

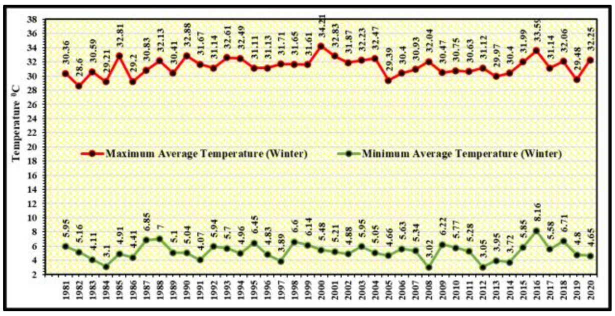


**Fig. 10.** Historical maximum and minimum average winter temperature from 1981-2020.

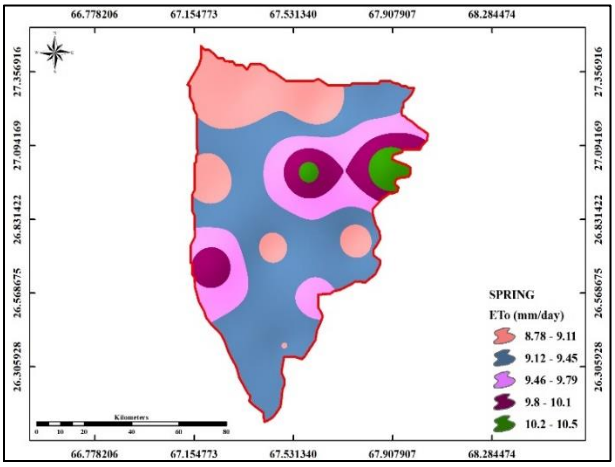


**Fig. 11.** Spring season ETo over the study area.

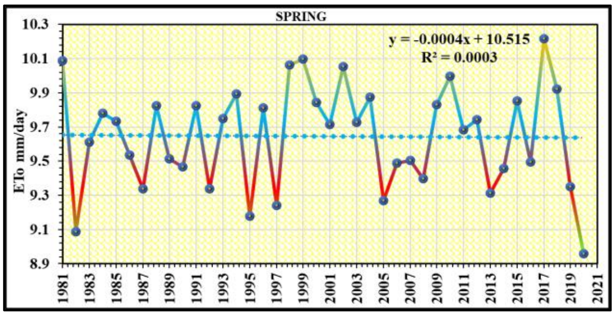


**Fig. 12.** Graph showing Spring season ETo from 1981-2021.

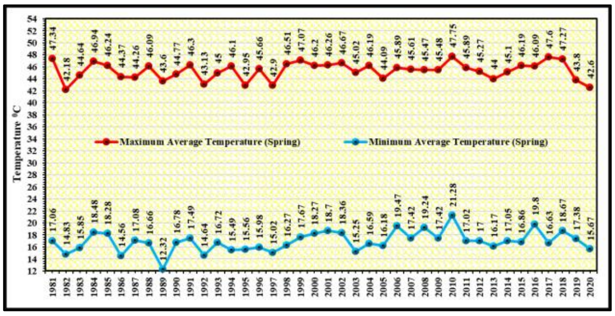


**Fig. 13.** Historical maximum and minimum average spring temperature from 1981-2020.

### 3.1.4. Summer reference evapotranspiration

The Summer season ETo was determined to range from 9.79 mm/day in 1981 and 9 mm/day in 2020. The trend line showed the value $R^2$=0.24 (Fig.15). The line showed there was a decrease in summer ETo from the past 39 years. The summer season ETo increased from southeast to northwest in the district. While agricultural land depicted the highest ETo calculated as 9.63 mm/day to 10.2 mm/day in the district (Fig. 14). On the other hand, hilly and mountain areas showed moderate ETo determined as 9.32-9.62 mm/day. The evapotranspiration in this season is depicted as high due to very high temperature and hot wind particularly called loo, which travels south to north throughout this season, especially in June and July month. The windiest month of the district is June with an average wind speed of 15.7 mph. However, (Fig. 14) shows the highest ETo recorded over the agricultural land, and values were determined between 9.95-10.2 mm/day.

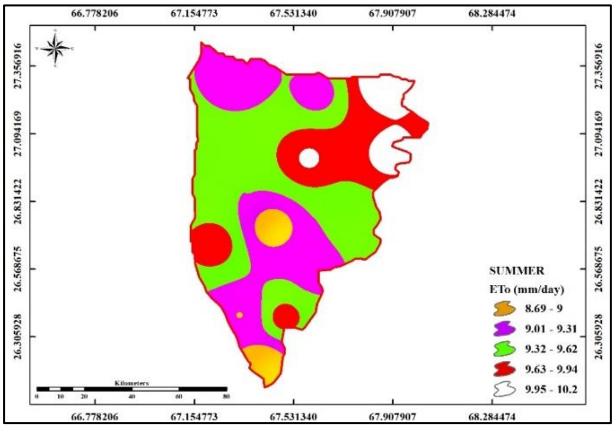


**Fig. 14.** Summer season ETo over the district.

### 3.1.5. Autumn reference evapotranspiration

The autumn season ETo calculated 8.53 mm/day in 1981 to 8 mm/day in 2020 (Table. 2). The highest ETo was 8.93 mm/day computed in 2001 over the vegetation land in the district. The trend line showed $R^2$=0.24 (Fig. 17). It was observed through the long-term ETo, that the surface temperature during different seasons was fluctuating. If the temperature is higher than ETo is observed as increased in the study area. This season included September, October, and November months.

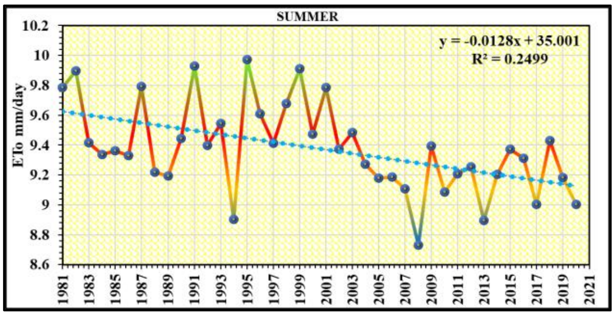


**Fig. 15.** Graph showing summer season ETo from 1981-2021.

September month always warms in the district and the evapotranspiration rate in the district was counted as high. The maximum ETo was determined over the vegetation area from 8.82 mm/day to 9.03 mm/day over the study area Dadu. The barren land area showed the lowest ETo from 8.15 mm/day to 8.36 mm/day (Fig. 16). The central part of the study area almost is barren land where surface water has been in limited quantity and due to less precipitation and shortage in canal water, this area always remains barren and uncultivated.

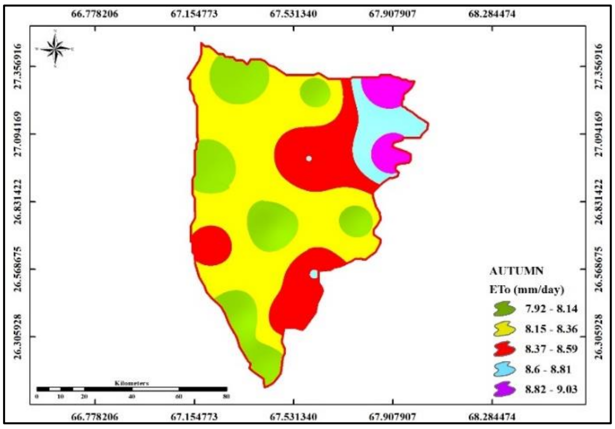


**Fig. 16.** Autumn ETo over the district.

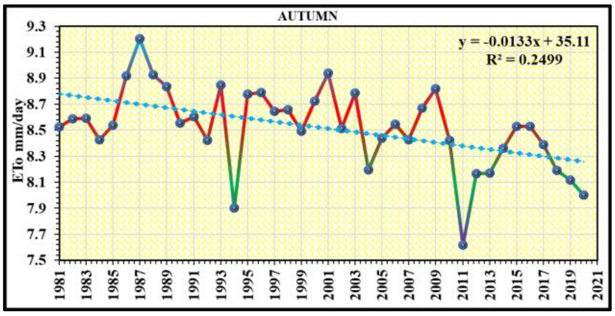


**Fig. 17**. Graph showing Autumn season ETo from 1981-2021.

### 3.2. Computation of historical monthly average ETo
#### 3.2.1. January reference evapotranspiration

The monthly average ETo results are demonstrated in (Fig. 18 & 19). Monthly January average ETo was computed ranging from 6.33 mm/day in 1981 and 6 mm/day in 2020. The maximum value of ETo in January depicted in 1990 was 7.06 mm/day. Whereas, the lowest value in January ETo was found at 5.52 mm/day in 2008. The trend line of ETo in January with $R^2$=0.0204 shows there was a decrease in annual ETo (Table. 3). The average temperature in this month lies between 25°C high and 9°C low. January month has seen low chances of rain on an average day. Historically, the Wind always blows at an average of between 7 to 8.4 mph in the January month in the study area.

**Table 2.** The long-term average annual and seasonal ETo (mm/day).

| YEAR | ANNUAL ETo | WINTER ETo | SPRING ETo | SUMMER ETo | AUTUMN ETo |
|---|---|---|---|---|---|
| 1981 | 8.76 | 6.64 | 10.09 | 9.79 | 8.53 |
| 1982 | 8.49 | 6.37 | 9.09 | 9.90 | 8.59 |
| 1983 | 8.65 | 6.78 | 9.61 | 9.42 | 8.59 |
| 1984 | 8.64 | 6.79 | 9.78 | 9.34 | 8.43 |
| 1985 | 8.85 | 7.51 | 9.73 | 9.36 | 8.54 |
| 1986 | 8.61 | 6.53 | 9.54 | 9.33 | 8.92 |
| 1987 | 8.84 | 6.93 | 9.34 | 9.79 | 9.20 |
| 1988 | 8.82 | 7.08 | 9.82 | 9.22 | 8.93 |
| 1989 | 8.67 | 6.86 | 9.51 | 9.19 | 8.83 |
| 1990 | 8.75 | 7.21 | 9.47 | 9.44 | 8.56 |
| 1991 | 8.94 | 7.19 | 9.82 | 9.93 | 8.60 |
| 1992 | 8.61 | 7.07 | 9.34 | 9.40 | 8.42 |
| 1993 | 8.91 | 7.30 | 9.75 | 9.54 | 8.85 |
| 1994 | 8.60 | 7.34 | 9.89 | 8.90 | 7.90 |
| 1995 | 8.68 | 6.75 | 9.18 | 9.97 | 8.78 |
| 1996 | 8.83 | 6.96 | 9.81 | 9.61 | 8.79 |
| 1997 | 8.66 | 7.09 | 9.24 | 9.41 | 8.64 |
| 1998 | 8.89 | 7.01 | 10.06 | 9.68 | 8.66 |
| 1999 | 8.92 | 7.06 | 10.10 | 9.91 | 8.49 |
| 2000 | 9.05 | 7.84 | 9.84 | 9.47 | 8.73 |
| 2001 | 8.99 | 7.33 | 9.71 | 9.78 | 8.94 |
| 2002 | 8.85 | 7.20 | 10.05 | 9.37 | 8.51 |
| 2003 | 8.91 | 7.40 | 9.73 | 9.48 | 8.79 |
| 2004 | 8.76 | 7.39 | 9.88 | 9.27 | 8.19 |
| 2005 | 8.43 | 6.61 | 9.27 | 9.18 | 8.44 |
| 2006 | 8.55 | 6.83 | 9.49 | 9.18 | 8.55 |
| 2007 | 8.55 | 6.96 | 9.50 | 9.11 | 8.43 |
| 2008 | 8.55 | 7.01 | 9.40 | 8.73 | 8.67 |
| 2009 | 8.70 | 6.68 | 9.83 | 9.39 | 8.82 |
| 2010 | 8.65 | 6.93 | 10.00 | 9.09 | 8.42 |
| 2011 | 8.40 | 6.91 | 9.68 | 9.21 | 7.61 |
| 2012 | 8.62 | 6.96 | 9.74 | 9.26 | 8.17 |
| 2013 | 8.38 | 6.80 | 9.31 | 8.90 | 8.17 |
| 2014 | 8.51 | 6.73 | 9.46 | 9.20 | 8.36 |
| 2015 | 8.80 | 7.26 | 9.85 | 9.37 | 8.53 |
| 2016 | 8.68 | 7.24 | 9.49 | 9.31 | 8.53 |
| 2017 | 8.74 | 7.00 | 10.22 | 9.00 | 8.39 |
| 2018 | 8.67 | 6.99 | 9.92 | 9.43 | 8.19 |
| 2019 | 8.33 | 6.47 | 9.35 | 9.18 | 8.12 |
| 2020 | 8.35 | 7.15 | 8.96 | 9.00 | 8.00 |

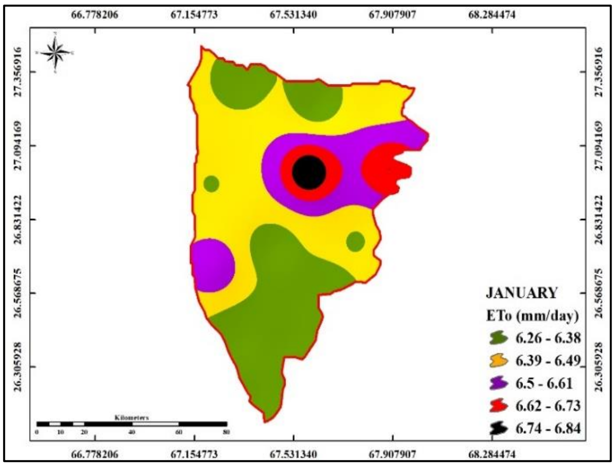


**Fig. 18**. January month ETo over the district.

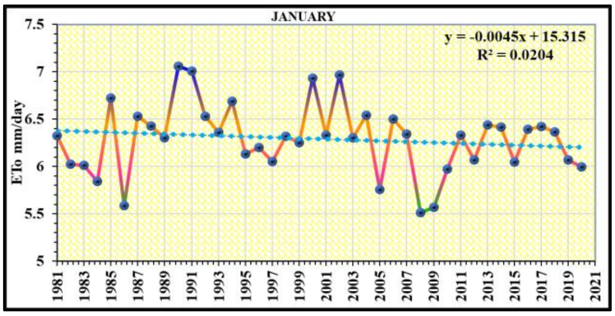


**Fig. 19.** Graph showing January ETo from 1981-2021.

#### 3.2.2. February reference evapotranspiration

Average ETo in February was computed ranging from 7.17 mm/day in 1981 and 7.79 mm/day in 2020. The maximum ETo in this month depicted in 1997 was 8.92 mm/day. Although, the lowest ETo in February was found at 6.32 mm/day in 2013 (Table. 3). The trend line of ETo in February with $R^2$=0.010 shows there was a decrease in annual ETo from the last 39 years (Fig. 21). The graphical representation of the Dadu district (Fig. 20) showed that the highest evapotranspiration lies over the mountains and hilly areas with 7.49-7.79 mm/day in February month. February counted as the cold month in the region with an average temperature between 28°C high and 11°C low.

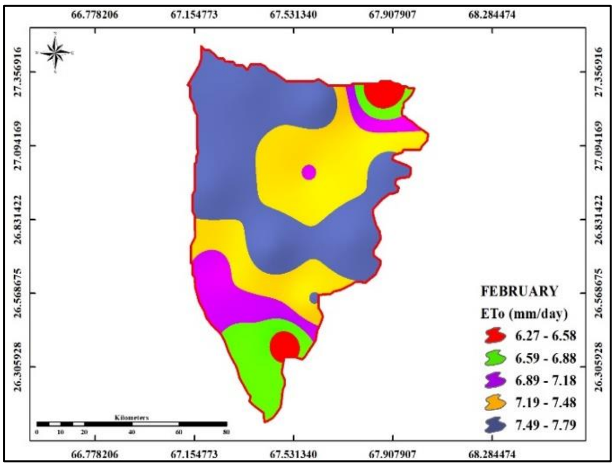


**Fig. 20.** February month ETo over the district.

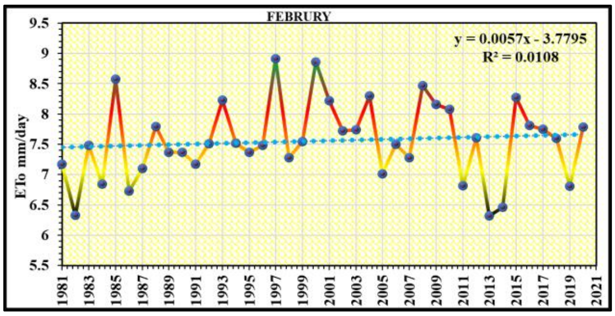


**Fig. 21**. Graph showing February ETo from 1981-2021.

#### 3.2.3. March reference evapotranspiration

The average values of ETo in march month computed as 9.13 mm/day in 1981 and 7.97 mm/day in 2020. The highest value of ETo observed in 1999 was 9.77 mm/day, while the lowest evapotranspiration determined in 1989 was 7.77 mm/day (Fig. 22). The trend line showed there was an increase in the ETo in March month as the value was recorded as $R^2$=0.014. (Fig. 23) shows that the highest ETo is depicted in the vegetative areas. On the other side, less ETo was seen over the hilly areas. The average temperature in this month was recorded between 33 °C to 16 °C.

#### 3.2.4. April reference evapotranspiration

The average ETo of April month was calculated ranging from 10.52 mm/day in 1981 and 9.14 mm/day in 2020 (Fig. 24). The linear coefficient value computed as $R^2$=0.014 showed there was a decrease in the ETo in 39 years of data (Fig. 25). The maximum evapotranspiration calculated in 1981 was 10.52 mm/day and the minimum value was calculated as 8.79 mm/day in 1995. The interpolated map of April month depicted that barren land and vegetation cover has moderate ETo with a calculated range between 9.18 mm/day to 10.1 mm/day over the study area. While on the north side of the district particularly in hilly areas was a very low ETo 8.73 mm/day to 9.17 mm/day.

#### 3.2.5. May reference evapotranspiration

In May, the coefficient value of ETo along the trend line was determined as $R^2$=0.0025 and pointed out a decreased trend from the past 39 years. (Table. 2 & Fig. 27) showed that the maximum value of ETo was 10.90 mm/day in 2010 and the minimum value in 1982 was 9.42 mm/day. Whereas, the maximum ETo in (Fig. 26), a little portion of vegetation which depicted 10.6 mm/day to 10.8 mm/day.

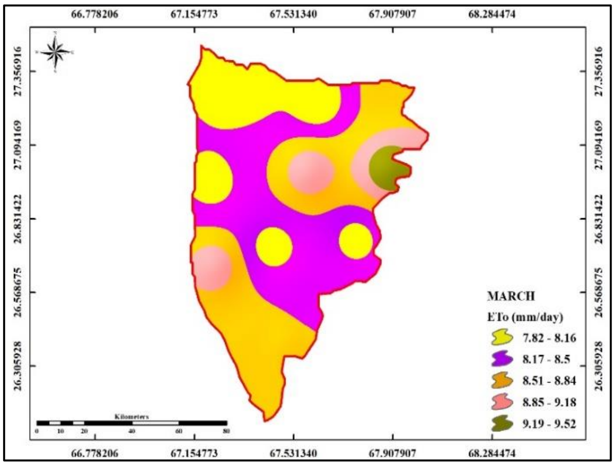


**Fig. 22.** March month ETo over the district.

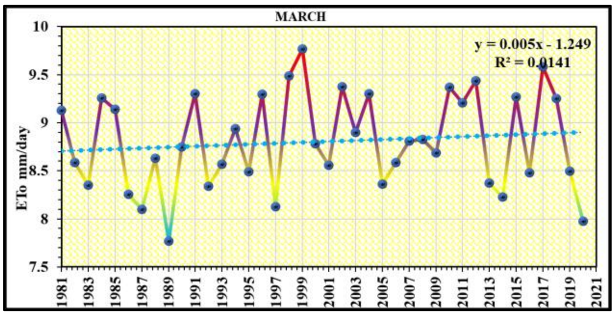


**Fig. 23.** Graph showing March ETo from 1981-2021.

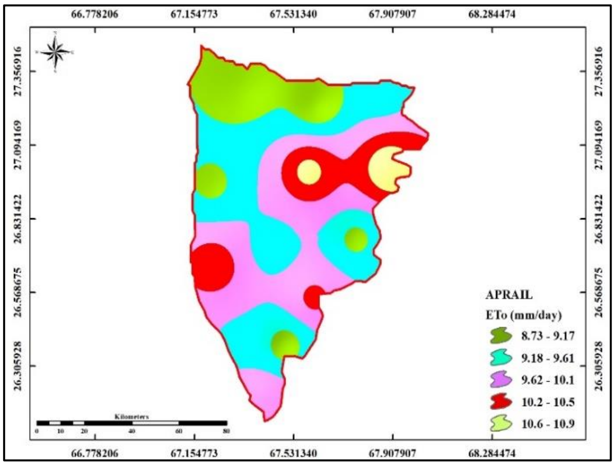


**Fig. 24.** April month ETo over the district.

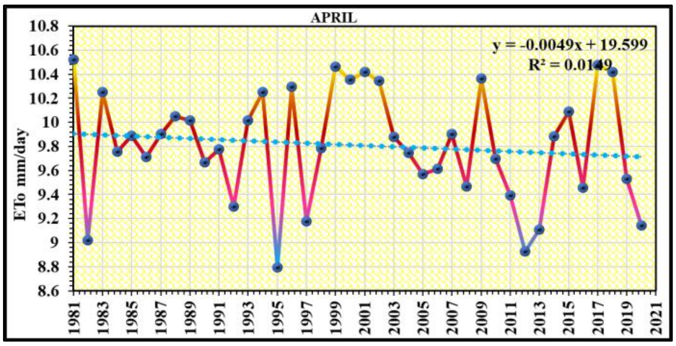


**Fig. 25.** Graph showing April ETo from 1981-2021.

The barren land area showed moderate ETo determined values between 9.9 mm/day to 10.2 mm/day. However, May month counted as warm and the average temperature recorded in the study area was 44 °C high and 27 °C low.

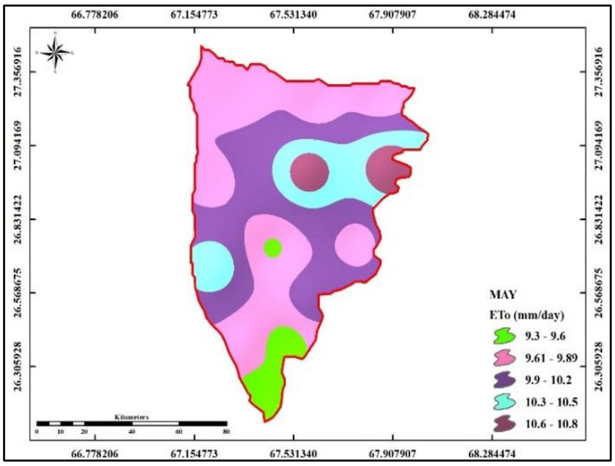


**Fig. 26.** May month ETo over the district.

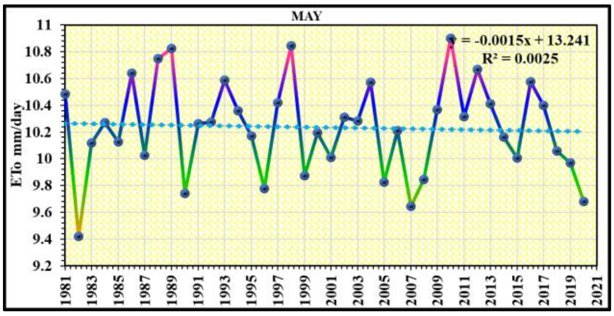


**Fig. 27.** Graph showing May ETo from 1981-2021.

### 3.2.6. June Reference Evapotranspiration

Historical computation of ETo in June month, the range computed 10.37 mm/day in 1981 and 9.16 mm/day in 2020. The $R^2$=0.186. it was observed that there was a decrease in evapotranspiration in 39 years (Fig. 29). The highest value of ETo was calculated in 1991 as 10.86 mm/day and the lowest value was 8.99 mm/day in 2008 (Table 2 and Fig. 28). The evapotranspiration increases east to the north in the study area due to the plain area and towards the flood plain. June is the hottest month with an average temperature of 44 °C high and 29 °C low in the study area. The maximum ETo recorded over the cropland areas is 10.4 mm/day to 11.2 mm/day. While the barren land and hilly areas have low ETo 9.41 mm/day to 9.85 mm/day.

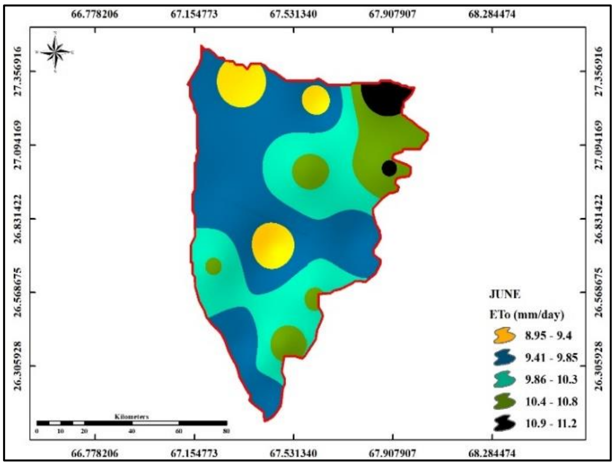


**Fig. 28.** June month ETo over the district.

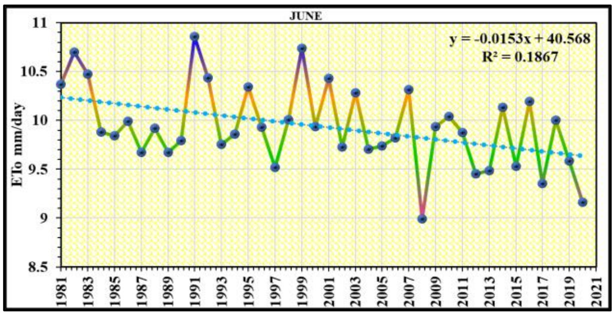


**Fig. 29**. Graph showing June ETo from 1981-2021.

### 3.2.7. July reference evapotranspiration

The ETo in July month ranged from 1981 to 2020 computed as 9.74 mm/day to 8.79 mm/day. The $R^2$=0.176 value was observed and showed a decreasing trendline of ETo from the last 39 years (Fig. 31). July month is the hottest in Pakistan, particularly in Sindh province which is plain by topography. The highest temperature in this month over the study area was recorded as 42°C. and the low average temperature of 22°C. (Fig. 30) showed that the moderate ETo values counted as 9.14 mm/day to 9.52 mm/day over the hilly and barren land. While the vegetative areas showed maximum ETo 9.93 mm/day to 10.3 mm/day.

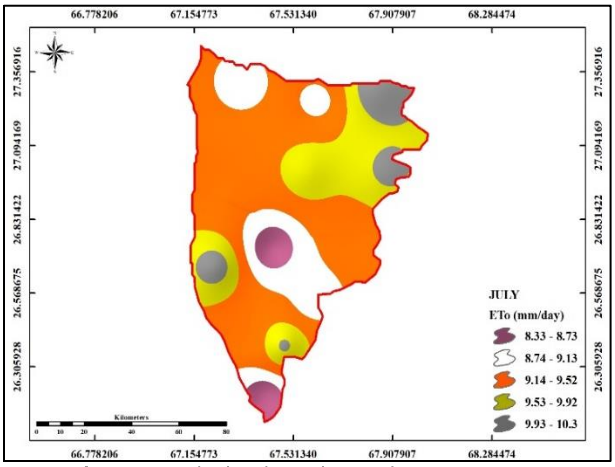


**Fig. 30**. Graph showing July ETo from 1981-2021.

### 3.2.8. August reference evapotranspiration

Historical average evapotranspiration values ranged from 1981 to 2020 computed as 9.2 mm/day to 9.03 mm/day in the August month (Table 2 & Fig. 32). The trend line showed there was a decrease in the ETo while $R^2$=0.0376 was determined in the study area (Fig. 33). The maximum ETo was calculated in 1987 as 9.88 mm/day. In the July and august months, the reference evapotranspiration increased from east to north and north to west.

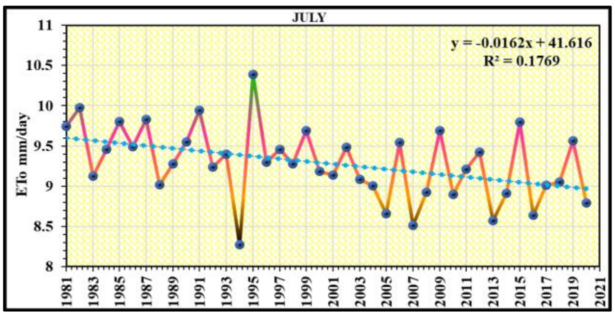


**Fig. 31.** Graph showing July ETo from 1981-2021.

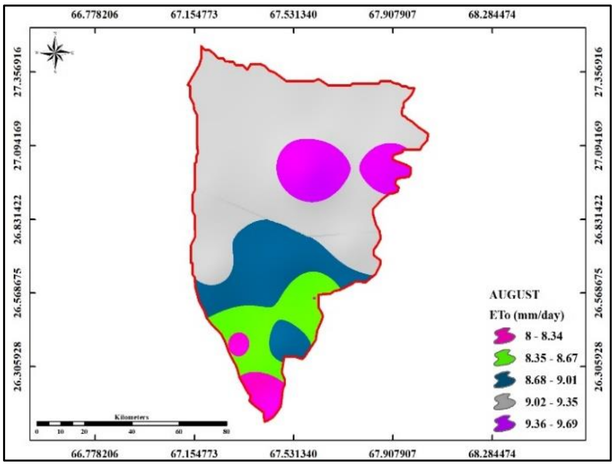


**Fig. 32.** August month ETo over the study area.

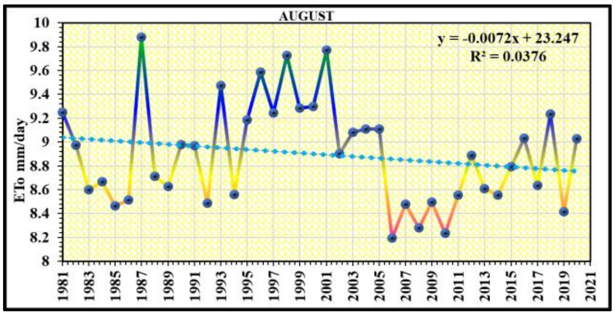


**Fig. 33.** Graph showing August ETo from 1981-2021.

### 3.2.9. September reference evapotranspiration

The month of September showed ETo range from 8.95 mm/day to 8.45 mm/day from 1981 to 2020. The maximum evapotranspiration was calculated using the derived equation as 10.14 mm/day in 1987 (Table. 2). The trend line showed there was a decrease in the ETo and $R^2$=0.224 was calculated (Fig. 35). The interpolated map (Fig. 34) depicted that there is less evapotranspiration on the barren land and hilly areas in the district. On the other hand, vegetative areas have high evapotranspiration calculated as 9.38 mm/day to 9.64 mm/day.

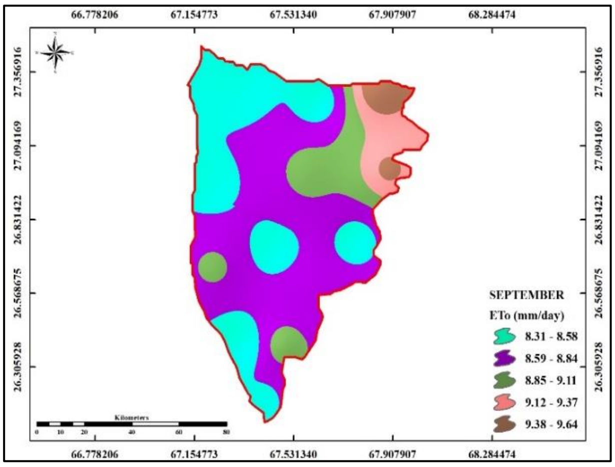


**Fig. 34.** September month ETo over the district.

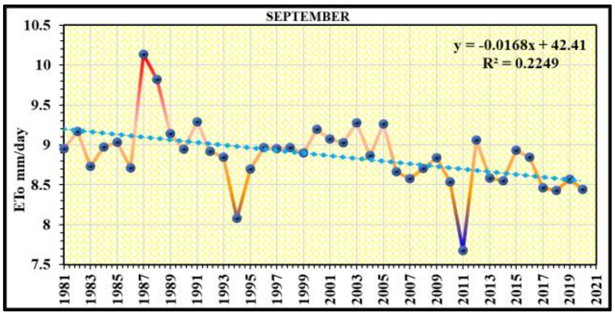


**Fig. 35.** Graph showing September ETo from 1981-2021.

### 3.2.10. October reference evapotranspiration

ETo in October computed as 8.80 mm/day in 1981 and 8.16 mm/day in 2020 (Table 2 and Fig. 36). $R^2$=0.1601 value was calculated. It is obvious from the linear regression line the ETo decreased in the last 39 years (Fig. 37). The maximum ETo calculated in 1983 was 9.44 mm/day. However, in the interpolation shown in (Fig. 36), The ETo depicted maximum over the vegetation and water surface bodies.

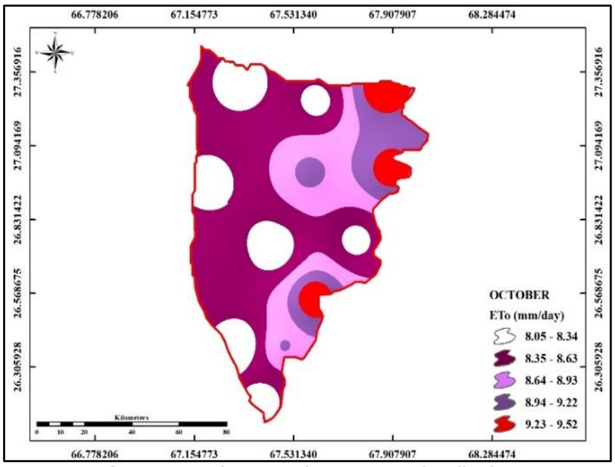


**Fig. 36.** October month ETo over the district.

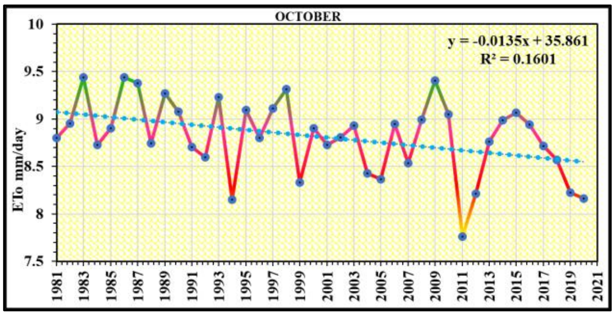


**Fig. 37.** Graph showing October ETo from 1981-2021.

### 3.2.11. November reference evapotranspiration

November month showed ETo range from 7.76 mm/day and 7.37 mm/day from 1981 to 2020 (Table. 2). The $R^2$=0.092 showed there was a decrease in evapotranspiration in the study area (Fig. 39). The highest ETo distinguished over the vegetation was 7.85 mm/day to 8.01 mm/day. While the barren land and some portion of the hilly areas have low evapotranspiration calculated from 7.36 mm/day to 7.51 mm/day in November. On the lakeside, ETo was determined as very low 7.19 mm/day to 7.35 mm/day due to low surface temperature and high humidity rate in the district (Fig. 38).

### 3.2.12. December reference evapotranspiration

Last month December showed ETo calculated range as 6.09 mm/day to 7.39 mm/day from 1981 to 2020. The trendline showed there was $R^2$=0.0049. Hence, ETo became increased from the previous 39 years (Fig. 41). The maximum value counted as 7.82 mm/day in 2003. In December, the ETo was determined as low 6.53 mm/day to 6.81 mm/day over the vegetation. December month is cold climatic parameters surface temperature and wind speed are recorded as low. While the humidity was noted as high this month. The results clearly showed the ETo values are less in the district.

The Hargreaves-Samani method was constructed particularly for the irrigation management, and planning of irrigation applications. The FAO—PM method was based on the on-site requirement, equipment, quality of weather data and availability, and calculation simplicity. Whereas these all requirements for the FAO-PM method were unavailable and questionable for ETo. Due to unavailability, FAO recommended this equation called the HS equation. The HS equation used in conjunction with NASA-POWER datasets and IDW interpolation with ArcMap 10.8 was all temperature-based, thus, their distribution patterns are to some extent interrelated to the distribution of the temperature. The equation formed a smoother and more gradual spreading of ETo results due to the complex terrain of the study area. This study exploited the IDW technique of interpolation as it is commonly the technique used when it comes to manipulating weatherrelated variables. IDW was a good choice due to auto-correlation and because it is an exact interpolation method, and for this reason, the IDW interpolation would have derived precise results. Regardless of the estimation of ETo for different periods in any place of the globe, NASA-POWER products are accurate, suitable, and reliable where most of the climate variables may not be easily approachable. The high altitude and plain area of the district have variations in the ETo. This is due to fluctuations in the climatic parameters like rainfall, high and low temperature over hilly and cropland areas, sunshine duration, atmospheric pressure as well as humidity, and wind speed. In the winter and summer seasons, along the river Indus, the evapotranspiration was recorded high as compared to hilly areas of the district. The intensity of the ETo is a result of natural phenomena but it might increase with the increase in vegetation cover, expansion in streams, cropping activities as well as in atmospheric pollution.

**Table 3**. Illustrate long term average monthly ETo (mm/day) in Dadu district.

| Year | January | February | March | April | May | June | July | August | September | October | November | December |
|---|---|---|---|---|---|---|---|---|---|---|---|---|
| 1981 | 6.33 | 7.17 | 9.13 | 10.52 | 10.48 | 10.37 | 9.74 | 9.25 | 8.95 | 8.80 | 7.76 | 6.09 |
| 1982 | 6.02 | 6.33 | 8.59 | 9.02 | 9.42 | 10.70 | 9.98 | 8.97 | 9.17 | 8.95 | 7.63 | 6.46 |
| 1983 | 6.01 | 7.48 | 8.35 | 10.25 | 10.12 | 10.47 | 9.12 | 8.60 | 8.73 | 9.44 | 7.52 | 6.54 |
| 1984 | 5.84 | 6.84 | 9.25 | 9.76 | 10.27 | 9.88 | 9.46 | 8.67 | 8.97 | 8.73 | 7.52 | 7.35 |
| 1985 | 6.73 | 8.57 | 9.14 | 9.89 | 10.12 | 9.84 | 9.80 | 8.47 | 9.04 | 8.90 | 7.62 | 6.93 |
| 1986 | 5.58 | 6.73 | 8.25 | 9.71 | 10.64 | 9.99 | 9.49 | 8.51 | 8.71 | 9.44 | 8.43 | 6.97 |
| 1987 | 6.53 | 7.10 | 8.10 | 9.90 | 10.03 | 9.67 | 9.83 | 9.88 | 10.14 | 9.38 | 8.09 | 6.84 |
| 1988 | 6.43 | 7.79 | 8.63 | 10.05 | 10.75 | 9.92 | 9.02 | 8.71 | 9.82 | 8.74 | 8.16 | 6.77 |
| 1989 | 6.30 | 7.36 | 7.77 | 10.02 | 10.82 | 9.67 | 9.28 | 8.63 | 9.14 | 9.27 | 8.02 | 6.70 |
| 1990 | 7.06 | 7.37 | 8.75 | 9.67 | 9.74 | 9.79 | 9.55 | 8.98 | 8.95 | 9.08 | 7.58 | 6.85 |
| 1991 | 7.01 | 7.17 | 9.30 | 9.78 | 10.26 | 10.86 | 9.95 | 8.97 | 9.29 | 8.71 | 7.78 | 7.03 |
| 1992 | 6.53 | 7.51 | 8.34 | 9.30 | 10.28 | 10.44 | 9.24 | 8.49 | 8.92 | 8.60 | 7.69 | 6.84 |
| 1993 | 6.36 | 8.23 | 8.57 | 10.01 | 10.59 | 9.76 | 9.40 | 9.47 | 8.85 | 9.23 | 8.35 | 6.99 |
| 1994 | 6.69 | 7.52 | 8.94 | 10.25 | 10.36 | 9.86 | 8.27 | 8.56 | 8.08 | 8.15 | 7.47 | 7.51 |
| 1995 | 6.13 | 7.37 | 8.49 | 8.79 | 10.17 | 10.34 | 10.39 | 9.18 | 8.69 | 9.10 | 8.24 | 6.43 |
| 1996 | 6.20 | 7.48 | 9.30 | 10.30 | 9.78 | 9.93 | 9.29 | 9.59 | 8.97 | 8.80 | 8.38 | 6.87 |
| 1997 | 6.05 | 8.92 | 8.12 | 9.18 | 10.42 | 9.52 | 9.46 | 9.25 | 8.95 | 9.11 | 7.75 | 6.22 |
| 1998 | 6.32 | 7.28 | 9.49 | 9.79 | 10.85 | 10.01 | 9.28 | 9.73 | 8.97 | 9.32 | 7.62 | 7.11 |
| 1999 | 6.25 | 7.55 | 9.77 | 10.46 | 9.87 | 10.74 | 9.69 | 9.28 | 8.90 | 8.33 | 8.17 | 7.13 |
| 2000 | 6.93 | 8.86 | 8.78 | 10.35 | 10.19 | 9.94 | 9.18 | 9.30 | 9.20 | 8.90 | 7.98 | 7.35 |
| 2001 | 6.33 | 8.22 | 8.56 | 10.42 | 10.01 | 10.43 | 9.14 | 9.77 | 9.07 | 8.73 | 8.90 | 7.15 |
| 2002 | 6.96 | 7.72 | 9.37 | 10.34 | 10.31 | 9.73 | 9.49 | 8.90 | 9.03 | 8.81 | 7.69 | 6.57 |
| 2003 | 6.30 | 7.74 | 8.90 | 9.88 | 10.28 | 10.28 | 9.09 | 9.08 | 9.27 | 8.93 | 8.09 | 7.82 |
| 2004 | 6.54 | 8.30 | 9.30 | 9.74 | 10.57 | 9.70 | 9.00 | 9.11 | 8.87 | 8.43 | 7.24 | 7.01 |
| 2005 | 5.76 | 7.01 | 8.36 | 9.57 | 9.83 | 9.74 | 8.66 | 9.11 | 9.26 | 8.36 | 7.59 | 6.76 |
| 2006 | 6.50 | 7.50 | 8.59 | 9.61 | 10.21 | 9.82 | 9.54 | 8.20 | 8.66 | 8.95 | 7.91 | 6.03 |
| 2007 | 6.34 | 7.28 | 8.81 | 9.90 | 9.65 | 10.31 | 8.51 | 8.48 | 8.58 | 8.53 | 8.10 | 6.87 |
| 2008 | 5.52 | 8.47 | 8.82 | 9.47 | 9.84 | 8.99 | 8.92 | 8.28 | 8.71 | 8.99 | 8.13 | 6.78 |
| 2009 | 5.57 | 8.15 | 8.69 | 10.36 | 10.37 | 9.94 | 9.69 | 8.50 | 8.84 | 9.40 | 8.06 | 6.03 |
| 2010 | 5.97 | 8.07 | 9.37 | 9.70 | 10.90 | 10.04 | 8.90 | 8.23 | 8.53 | 9.05 | 7.62 | 6.38 |
| 2011 | 6.33 | 6.81 | 9.21 | 9.39 | 10.31 | 9.88 | 9.21 | 8.55 | 7.68 | 7.76 | 7.36 | 7.23 |
| 2012 | 6.07 | 7.61 | 9.43 | 8.93 | 10.67 | 9.45 | 9.42 | 8.89 | 9.06 | 8.21 | 7.24 | 6.87 |
| 2013 | 6.44 | 6.32 | 8.37 | 9.11 | 10.41 | 9.49 | 8.57 | 8.61 | 8.58 | 8.76 | 7.11 | 7.31 |
| 2014 | 6.42 | 6.46 | 8.23 | 9.88 | 10.16 | 10.13 | 8.91 | 8.55 | 8.55 | 8.99 | 7.46 | 6.97 |
| 2015 | 6.05 | 8.27 | 9.27 | 10.09 | 10.01 | 9.53 | 9.80 | 8.80 | 8.94 | 9.07 | 7.56 | 7.22 |
| 2016 | 6.39 | 7.81 | 8.48 | 9.46 | 10.58 | 10.19 | 8.64 | 9.03 | 8.84 | 8.94 | 7.73 | 7.15 |
| 2017 | 6.42 | 7.75 | 9.58 | 10.48 | 10.40 | 9.35 | 9.01 | 8.63 | 8.47 | 8.72 | 7.84 | 6.52 |
| 2018 | 6.36 | 7.60 | 9.25 | 10.42 | 10.06 | 10.00 | 9.05 | 9.24 | 8.43 | 8.57 | 7.55 | 6.70 |
| 2019 | 6.07 | 6.81 | 8.49 | 9.53 | 9.97 | 9.59 | 9.56 | 8.41 | 8.57 | 8.22 | 7.39 | 6.20 |
| 2020 | 6.00 | 7.79 | 7.97 | 9.14 | 9.68 | 9.16 | 8.79 | 9.03 | 8.45 | 8.16 | 7.37 | 7.39 |

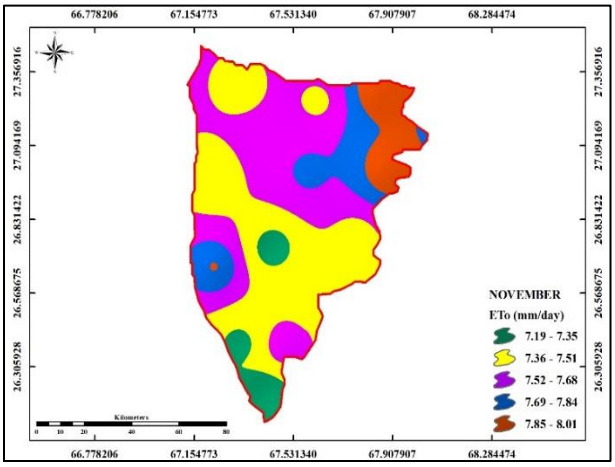


**Fig. 38.** November month ETo over the district.

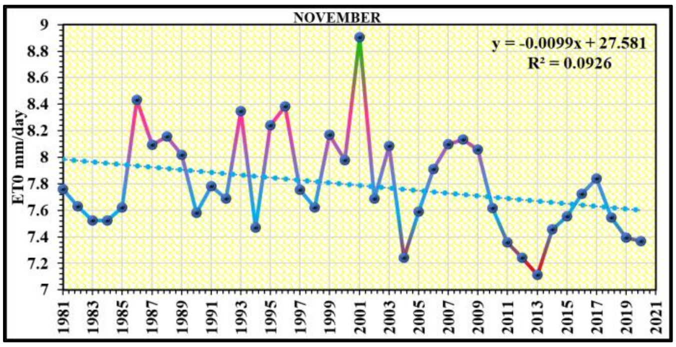


**Fig. 39.** Graph showing November ETo from 1981-2021.

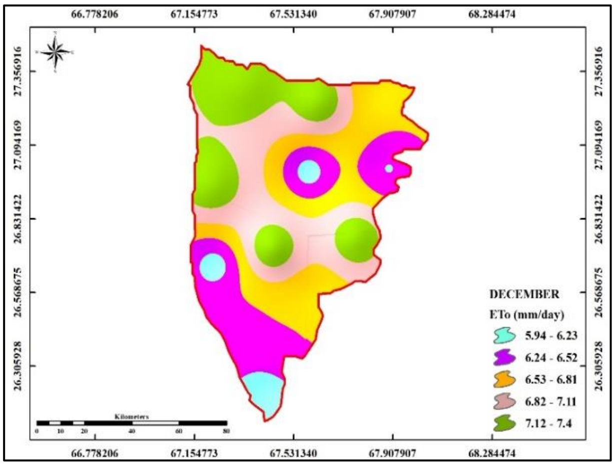


**Fig. 40.** December month ETo over the district.

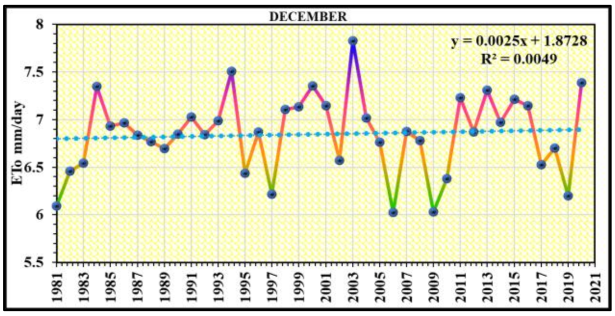


**Fig. 41**. Graph showing December ETo from 1981-2021.

## 4. Conclusions

The accurate estimation of ETo plays a significant role in decision support for WMR, design, and scheduling of irrigation systems, crop efficiency, and water productivity. However, some techniques for the estimation of ETo require a wide range of data. While, simpler methods, only data on maximum and minimum air temperature and extraterrestrial radiation. Based on the results, the HS technique can be used to estimate annual, seasonal, and monthly ETo in any region. Due to the simplicity of the equation. The study has evaluated the accuracy of the temperature-based equation to estimate the ETo in the Dadu district. On the other hand, the spatial distribution of ETo displaying, aid in water resource planning and management. It allows a historical comparison of spatial mapping to estimate if ETo rates are shifting from one direction to another. It also assists in environmental hazards planning including drought, and forest fires, and supports risk management strategies for the policymakers in developing regions.

Thus, GIS and RS have been particularly used as influential tools in which Spatio-temporal assessment and integration of environmental along with ecological variables continues to rise. Though, this study provides a simple and efficient technique to spatially estimate historical ETo rates annual, seasonal and monthly basis with the support of the POWER data in ArcGIS 10.8. Therefore, a large number of datasets must initially be pre-processed in MS Excel format. A temperature-based equation like HS should be selected for ETo calculation due to limited data as input. The choice of selecting the interpolation method is another technique that has the potential for extension. This study not only relies on the HS equation for ETo but also focuses on the specific IDW interpolation for the spatial distribution of ETo. However, ArcGIS 10.8 enables us to calculate more accurate ETo efficiently because only simple input and output maps are needed for annual, seasonal, and monthly ETo.

## References

Allen R.G., Pereira L.S., Raes D., Smith M., Crop Evapotranspiration; guidelines for computing crop water requirements-FAO-Irrigation and Drainage paper N 56. Food and Agriculture Organization of the United Nation. Rome; Italy; (1998), p. 20.

Chandler W.S., Hoell J.M., Westberg D., Zhang T., and Stackhouse P.W., Jr., NASA prediction of worldwide energy resource high-resolution metrology data for sustainable building design. In proceedings of the Solar 2013 conference of American Solar Energy Society, Baltimore, MD, USA, 16-20 April (2013).

Droogers P., and Allen R.G., Estimating ETo under inaccurate data conditions, Irrigation and Drainage Systems 16 (2002) 33-45.

Gentilucci M., Bufalini M., Materazzi M., Barbieri M., Aringoli D., Farabollini P., Pambianchi G., Calculation of potential evapotranspiration and calibration of the Hargreaves equation using Geostatistical methods over the last 10 years in central Italy, Geoscience 11 (2021) 348.

Hargreaves G.H., and Samani Z.A., Reference crop ETo from temperature, Applied Engineering in Agriculture 1 (1995) 96-99.

Khan S., and Hasan U.H., Evapotranspiration distribution and variation of Pakistan (1931-2015), Annals of Valahia University of Targovishte Geographical Series 17 (2) (2017) 184-197.

Kobayashi S., Ota Y., Harada Y., Ebita A., Moriya M., Onoda H., Onogi K., Kamahori H., Kobayashi C., Miyaoka, K., Takahashi K., The JRA-55 reanalysis: General specifications and basic characteristics. Journal of Meteorological Society of Japan. Ser. II. 93 (2015) 5-48.

Pakistan Bureau of Statistics, Final results of Census-2017. https://www.pbs.gov.pk/sites/default/files/population/2017/sindh_district_wise.pdf. (Accessed 13 March 2021).

Rodrigues G.C., and Braga R.P., Estimation of daily ETo from NASA-POWER reanalysis products in a hot-summer Mediterranean climate. Agronomy 11 (2021) 2077.

Shiri J., Evaluation of a neuro-fuzzy technique in estimating pan evaporation values in low-altitude locations, Metrological Applications 26 (2019) 204-212.

Tabari H., Grismer M.E., and Trajkovic S., Comparative analysis of 131 ETo methods under humid conditions, Irrigation Science 31 (2013) 107-117.

Thornthwaite C.W., An approach toward a rational classification of climate, Geographical Review 38 (1948) 55-94.

Xu C.Y., and Singh V., Cross comparison of empirical equations for calculating potential evapotranspiration with data from Switzerland, Water Resources Management 16 (2002) 197-219.

Yamac S.S., Estimation of long-term ETo using limited weather data in sugar beet plantation area from middle Anatolian, Turkey, Journal of Faculty of Agriculture (2018) 160-165.